Vibrational Overtone Spectroscopy of Saturated Hydrocarbons Dissolved in Liquefied Ar, Kr, Xe, and N_2

Alfredo Lopez-Calvo and Carlos E. Manzanares*

Department of Chemistry & Biochemistry, Baylor University, 101 Bagby Avenue, Baylor Sciences Building E-216, Waco, Texas 76706

Received: August 27, 2007; In Final Form: December 8, 2007

This article presents a collection of vibrational overtone spectra of hydrocarbons in cryogenic solutions. Vibrational overtone spectra of ethane and propane dissolved in liquid argon and *n*-butane and isobutane dissolved in liquid krypton were recorded between 5000 and 14 000 cm^{-1}. Spectral regions for the first four overtones were measured using a Fourier transform spectrophotometer. The fifth overtone ($\Delta v = 6$) spectra were recorded with a double beam (pump−probe) thermal lens technique using concentrations as low as 10^{-3} mole fraction. We obtained the C−H ($\Delta v = 6$) spectra of (a) liquid ethane at 100 K and ethane in solutions in liquid Ar at 92 K and liquid N_2 at 85 K, (b) liquid propane at 148 K and propane in liquid Ar at 93 K, (c) *n*-butane in liquid Kr at 129 K, (d) *n*-pentane in liquid Xe at 160 K, and (e) isobutane liquid at 135 K and isobutane in liquid Kr at 130 K. Local-mode parameters were calculated for primary, secondary, and tertiary C−H oscillators in solution and compared with gas-phase local-mode parameters. The peak frequency shift ($\Delta\omega$) from gas phase to solution is explained by the change in harmonic frequency and anharmonicity in solution with respect to the gas-phase values. The bandwidth ($\Delta\omega_{1/2}$) of the ($\Delta v = 6$) C−H absorption bands of ethane in solution can be explained in terms of collisions with the solvent molecules.

1. Introduction

Liquefied rare gases exhibit particular advantages for low-temperature vibrational spectroscopy. They seem to produce minimal perturbations on the internal degrees of freedom of the dissolved molecules. Second, their high transparency in a broad spectral range allows the use of long path lengths, favoring quantitative studies of weak transitions, band shapes, and ro-vibrational relaxation in liquids. Third, optical homogeneity and high optical breakdown threshold make them suitable for nonlinear spectroscopy studies. And last, they offer the possibility of monitoring spectra over a broad range of temperature−density variation, necessary to obtain thermodynamic parameters of the solute−solvent and solute−solute interaction equilibria.[1,2] On the other hand, the main limitation of these solvents is the reduced solubility of the majority of molecular compounds. As a result, weak vibrational transitions only observed in high concentrations of the solute cannot be measured with absorption spectroscopy. Application of photoacoustic and photothermal techniques has overcome the issue. Their higher sensitivity has allowed the observation of the visible spectrum of several cryogenic solutions, as well as that of pure samples. Recently, Manzanares et al. reported the first application of thermal lensing to the field. The fifth overtone of methane−argon and methane−nitrogen solutions was obtained, decreasing the previous detection limit in concentration by a factor of 100.[3,4] The thermal lens technique used in our laboratory was originally introduced by Swofford et al.[5,6] to study vibrational overtones of liquid samples at room temperature.

The main contributions to high vibrational overtone studies in cryogenic liquids have been made by Patel et al.[7−10] and Manzanares et al.[11−16] Patel et al. used photoacoustic detection for the first time to measure high energy overtones ($\Delta v = 4-6$) of condensed methane,[7] ethylene,[8] and solid *para*-hydrogen.[9,10] Even though only pure samples were studied, Patel et al. showed the suitability of photoacoustic methods to measure overtones at low temperatures. Similarly, Manzanares et al. applied photoacoustic spectroscopy to cryogenic samples; however, they also prepared solutions in condensed argon. Some examples of their work include methane,[11] deuterated methanes,[12,13] ethylene,[14] and isobutane.[15] The limit of sensitivity was set by the fifth overtone of a methane (10%)−argon mixture.

Taking advantage of the excellent sensitivity shown by thermal lensing, we explore in this article the use of the technique to measure ($\Delta v = 6$) C−H overtone transitions of saturated hydrocarbons in cryogenic solutions of mole fraction around 0.1% (1000 ppm). Studies at low concentrations are important to observe the behavior of the molecule in situations where there are fewer interactions between solute molecules and where the solute is surrounded only by solvent molecules. The gas−solution frequency shift $\Delta\omega$ and the vibrational half-width $\Delta\omega_{1/2}$ are experimental parameters that are useful to theories of vibrational relaxation in liquids. In general, $\Delta\omega$ and $\Delta\omega_{1/2}$ change with temperature (T), density of the solvent (ρ), and vibrational quantum number (v) of the excited upper state. The reaction field model of solvation[17−19] assumes very dilute solutions where the molecules (monomers) absorb electromagnetic radiation surrounded only by a solvent with dielectric constant (ϵ). Infrared and Raman studies of fundamental transitions are possible, but vibrational overtone transitions in dilute solutions require the use of more sensitive techniques. Infrared studies of methane in solid *para*-hydrogen[20,21] have shown that methane monomers are only present when the concentration of methane is around or below 0.005% mole fraction (50 ppm), while dimers, trimers, and larger clusters begin to appear at higher concentrations. Our experiments have shown that vibrational fundamental and overtone study of

* Corresponding author. E-mail: Carlos_Manzanares@baylor.edu.

10.1021/jp076843v CCC: $40.75
Published on Web 02/02/2008

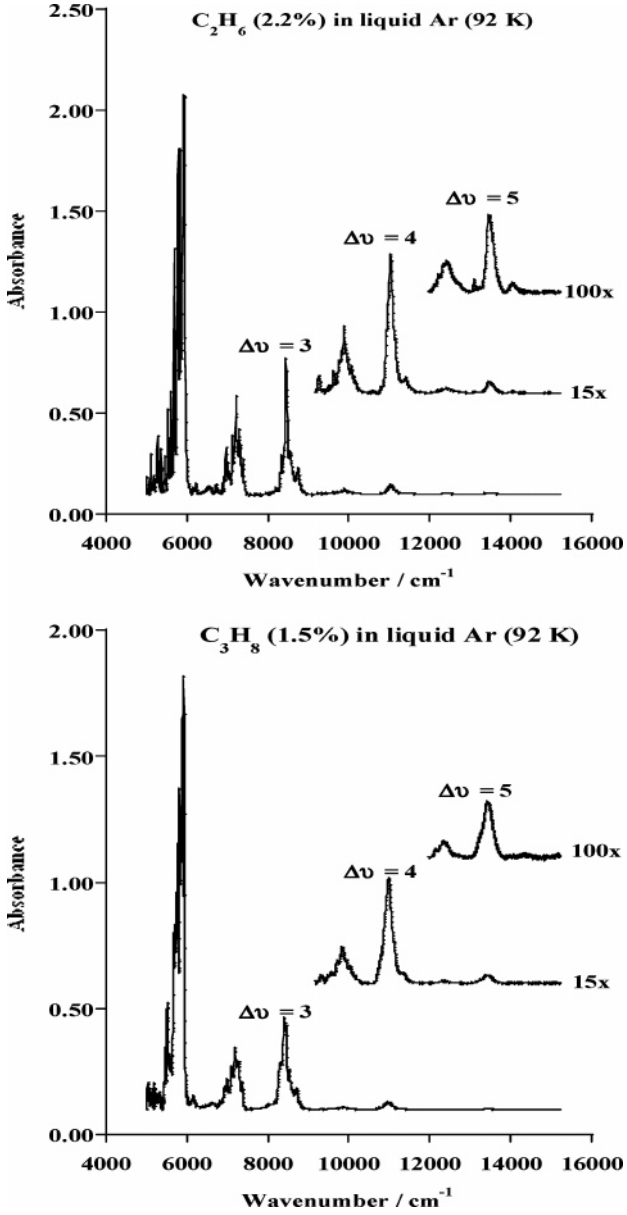

Figure 1. FT-NIR vibrational overtone spectra of C_2H_6 (2.2%) and C_3H_8 (1.5%) in liquid argon solutions at 92 K. Optical path length of 3.8 cm.

methane monomers in solution is possible up to $\Delta v = 6$ using thermal lens because our limit of detection for $\Delta v = 6$ is 54 ppm. In this article, we present a new contribution to the field of cryospectroscopy with a vibrational overtone study of several hydrocarbons in cryogenic solvents.

2. Experimental Section

The experimental techniques for vibrational overtone studies in cryogenic liquid solutions have been presented in a previous publication.[4] Low C−H vibrational overtones ($\Delta v = 2$, 3, 4, and 5) were obtained with a Fourier transform spectrophotometer (Thermo Nicolet, Nexus 670, 1 cm^{-1} resolution) operating in the near-infrared and visible regions of the electromagnetic spectrum. The $\Delta v = 6$ absorption bands were obtained with a double beam thermal lens technique. A dye laser (Coherent, 699, 1 cm^{-1} resolution) operating in the 603−660-nm region (laser dye Kiton red) was used to pump the molecules to the C−H ($\Delta v = 6$) vibrational level. An argon ion laser operating at 488 nm was used as the probe laser. Samples of different concentrations were prepared and stored in a lecture bottle. The mixtures were condensed in a cell attached to a low-temperature cryostat.

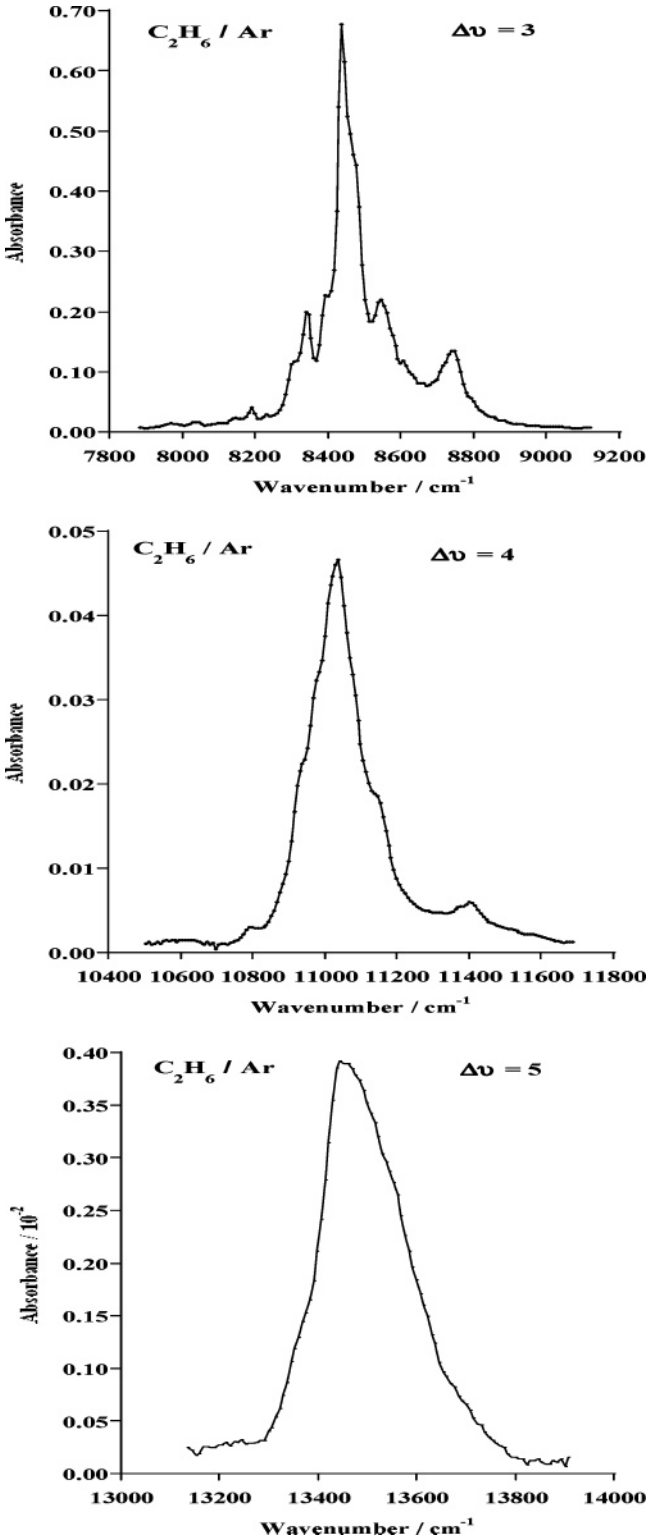

Figure 2. Selected absorption regions of vibrational C−H overtone spectra ($\Delta v = 3$, 4, 5) of C_2H_6 in liquid argon solution (2.2%) at 92 K.

3. Results

The Fourier transform near-infrared spectra of C_2H_6 (2.2%) and C_3H_8 (1.5%) in liquid argon solution are shown in Figure 1. The optical path length was 3.8 cm and the temperature 92 K. Four different spectral regions can be easily distinguished

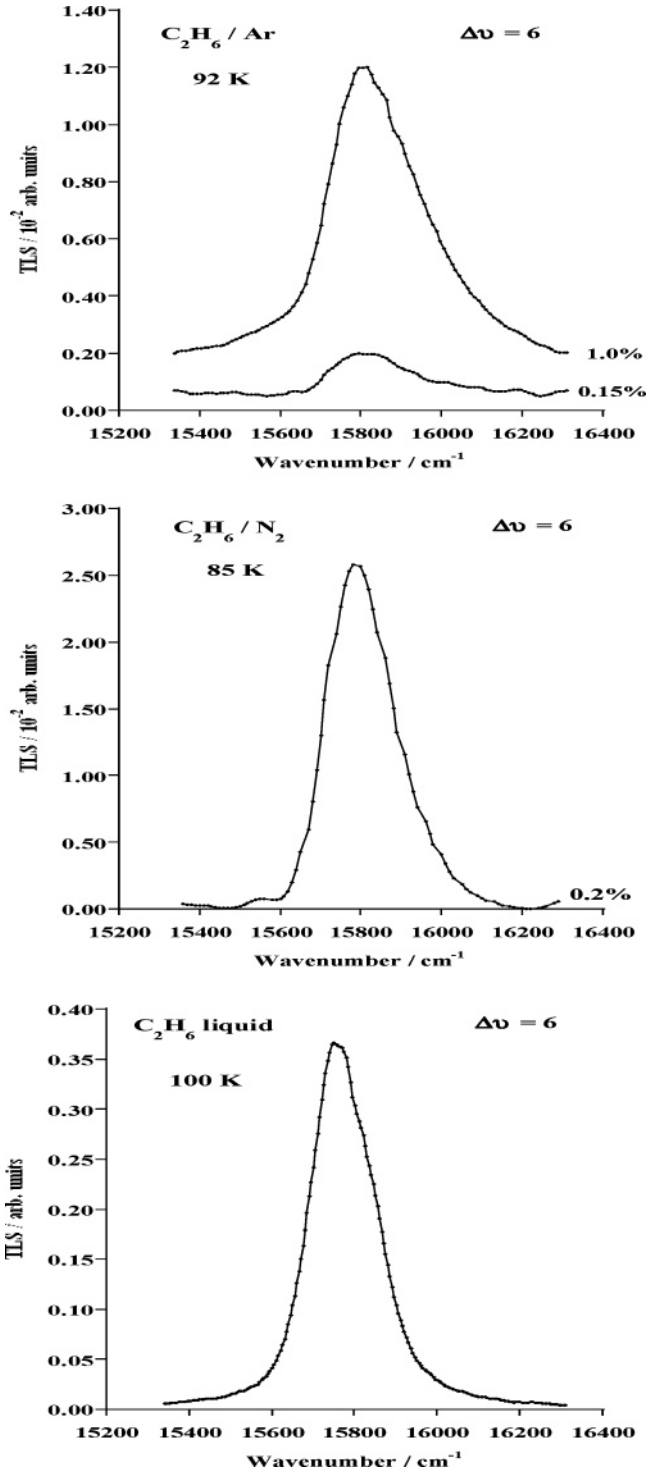

Figure 3. Thermal lens C−H ($\Delta v = 6$) spectra of C_2H_6 in liquid argon (92 K) at two different concentrations: 1.0 and 0.15%. Excitation powers of 20 and 100 mW, respectively (top). Thermal lens C−H ($\Delta v = 6$) spectrum of C_2H_6 in liquid nitrogen solution (0.2%) at 85 K and spectrum of liquid C_2H_6 at 100 K.

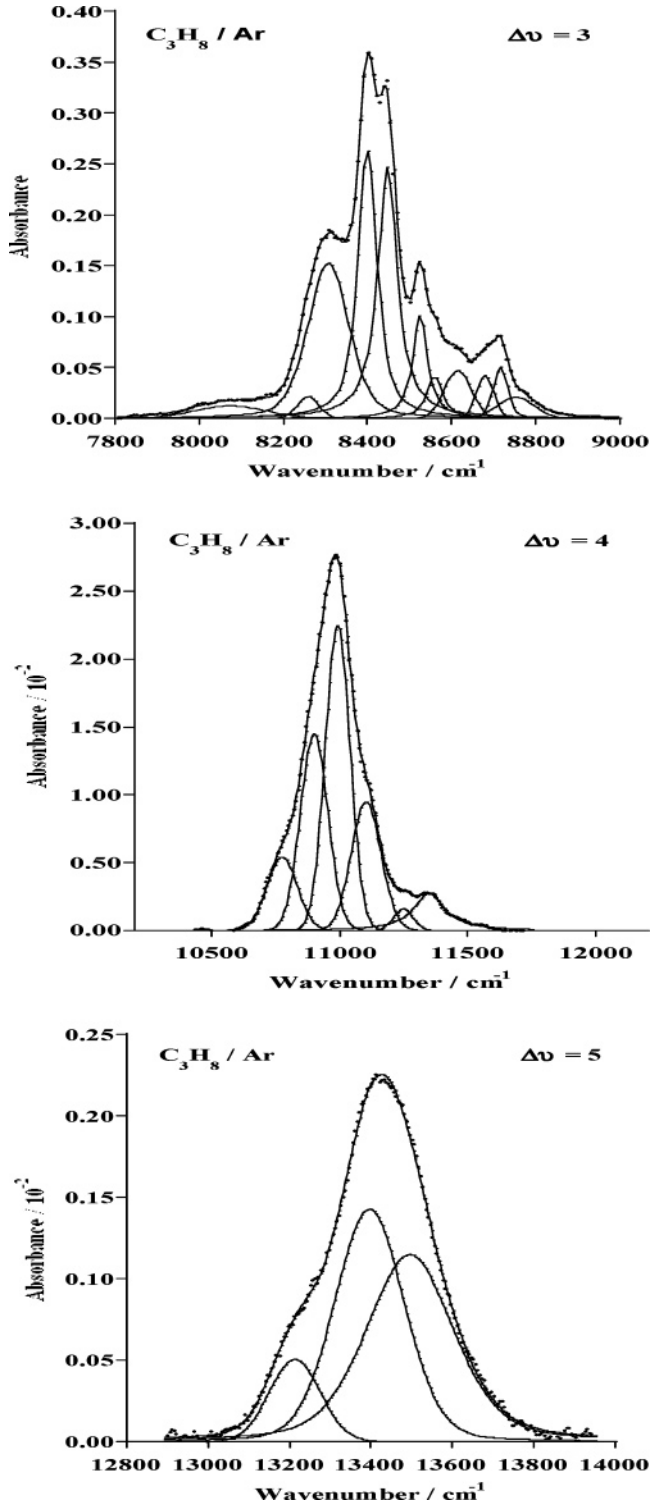

Figure 4. Selected absorption regions of vibrational C−H overtone spectra ($\Delta v = 3, 4, 5$) of C_3H_8 in liquid argon solution (2.2%) at 92 K.

with decreasing intensity. The first overtone lies below 6000 cm^{-1}, in a region heavily populated by combination bands. Transitions associated with absorption of three quanta of vibrational energy span from 7000 to 8500 cm^{-1}. A manifold of combination bands precedes the main overtone feature, and the pattern is repeated thereafter. The third overtone region extends from 9500 to 11 500 cm^{-1}; an amplification factor of 15 was necessary to show details of the absorption band. Finally, the region between 12 000 and 15 000 cm^{-1} contains the fourth overtone. Since this transition is very weak, a magnification factor of 100 was necessary to bring out the spectrum from the baseline.

Ethane. Individual overtone regions of C_2H_6 in liquid Ar are presented in Figure 2. The first overtone was not included since it usually does not follow the local-mode model, and spectral congestion makes it difficult to correctly assign the pure transition. Unlike that of heavier hydrocarbons, the spectrum of ethane is characterized by asymmetric bands with little or no structure. For this reason, no attempt was made to perform deconvolution of the bands. Correct assignment of experimental

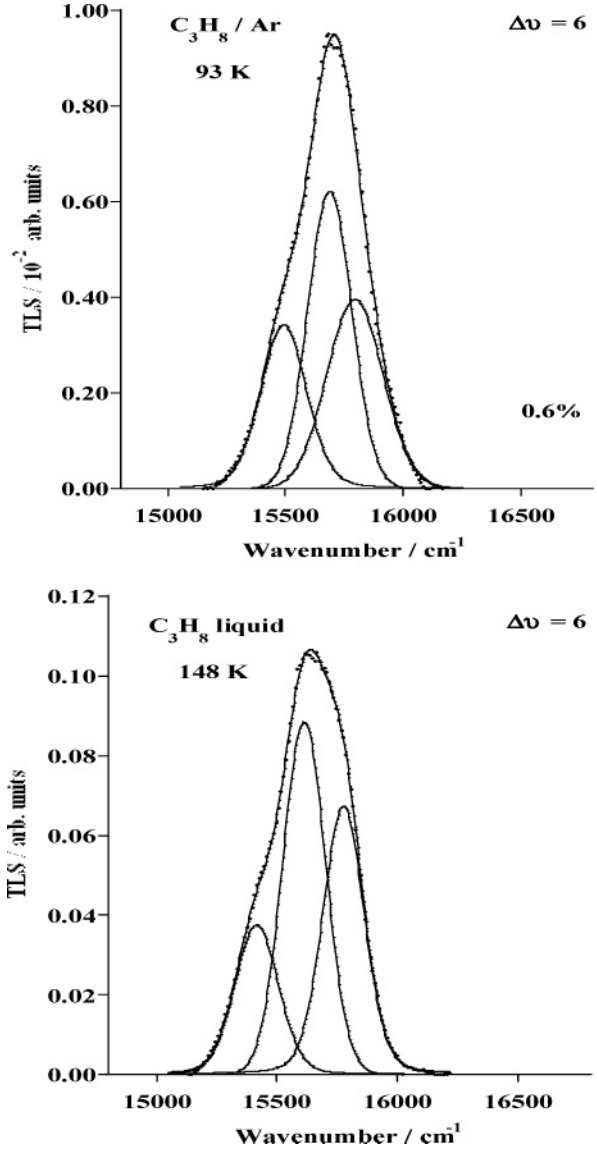

Figure 5. Thermal lens C−H ($\Delta v = 6$) spectrum of C_3H_8 in liquid argon solution (0.6%) at 92 K (top) and spectrum of liquid C_3H_8 at 148 K (bottom).

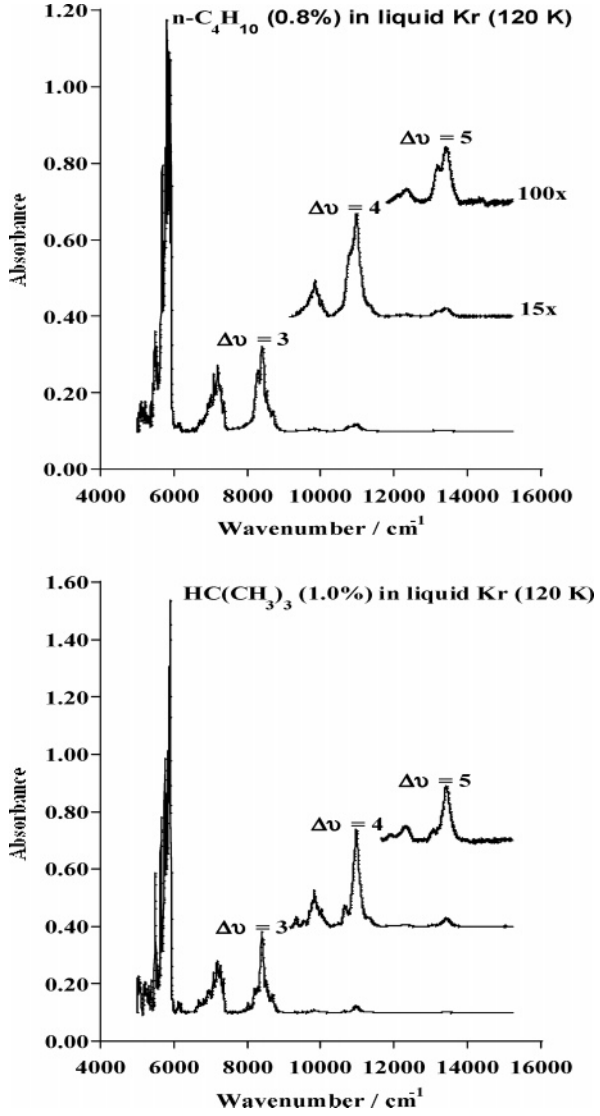

Figure 6. FT-NIR vibrational overtone spectra of *n*-C_4H_{10} (0.8%) (top) and $HC(CH_3)_3$ (1.0%) (bottom) in liquid krypton at 120 K.

bands was verified by comparison to previous reports in gas phase.[22−24] Even though Henry and Greenlay[24] carried out deconvolutions, high uncertainty is associated with the number of individual bands. For instance, only one band was assigned to the main peak in the third overtone region. By inspection of Figure 2 ($\Delta v = 4$), shoulders on this band indicate that at least four bands are necessary. To avoid ambiguity, each local-mode stretching overtone was assigned to the corresponding band maximum.

The spectra obtained using a thermal lens for ethane−argon solutions are shown in Figure 3. The C−H ($\Delta v = 6$) overtone spectrum was obtained for both C_2H_6 (0.15%)−Ar and C_2H_6 (1.0%)−Ar at 92 K. In the first case, the laser excitation power was 20 mW, and the chopping frequency was 7.0 Hz. In the second case, laser excitation was carried out at 100 mW and a chopping frequency of 5.0 Hz. The band is located at 15 775 cm^{-1}, and its full width at half-maximum (fwhm) is 270 cm^{-1}. The advantage of using the thermal lens is clearly demonstrated here by observing the enhancement in spectral features. No previous report of this band in condensed phase was found in the literature. Additional C−H ($\Delta v = 6$) thermal lens spectra are presented in Figure 3 where the spectrum of ethane dissolved in liquid nitrogen at 85 K is shown. The molar concentration of the gas mixture was 0.2%, the excitation power was 100 mW, and the chopping frequency was 7.0 Hz. The band is located at 15 776 cm^{-1}, and its width is 185 cm^{-1}. The spectrum of liquid ethane at 100 K is also shown. The band is located at 15 746 cm^{-1}, and its $\Delta\omega_{1/2}$ is 180 cm^{-1}.

Propane. The C−H overtone spectra of propane ($\Delta v = 3$, 4, and 5) in liquid argon are presented in Figure 4. To separate and assign individual bands, the spectra were deconvoluted with a product function having a predominant Lorentzian character perturbed by a small Gaussian function. The concentration of the sample was estimated to be 1.5%. As previously indicated for ethane, the optical path length was 3.8 cm and the liquid solution temperature was 92 K. The main difference between the spectra of propane and ethane is the presence of three nonequivalent C−H oscillators in the former. The corresponding analysis of overtones must be for individual C−H bonds, in contrast to the equivalent treatment given in ethane. Two different oscillators are found in a methyl group of propane. Bonds that align with the plane containing carbon atoms are labeled $C-H_{ip}$ (in-plane), while those that fall out of plane are labeled $C-H_{op}$ (out-of-plane). Methylene bonds are another kind, and they are labeled $C-H_m$. The energy order is known to be $C-H_m < C-H_{op} < C-H_{ip}$.[25] According to McKean et

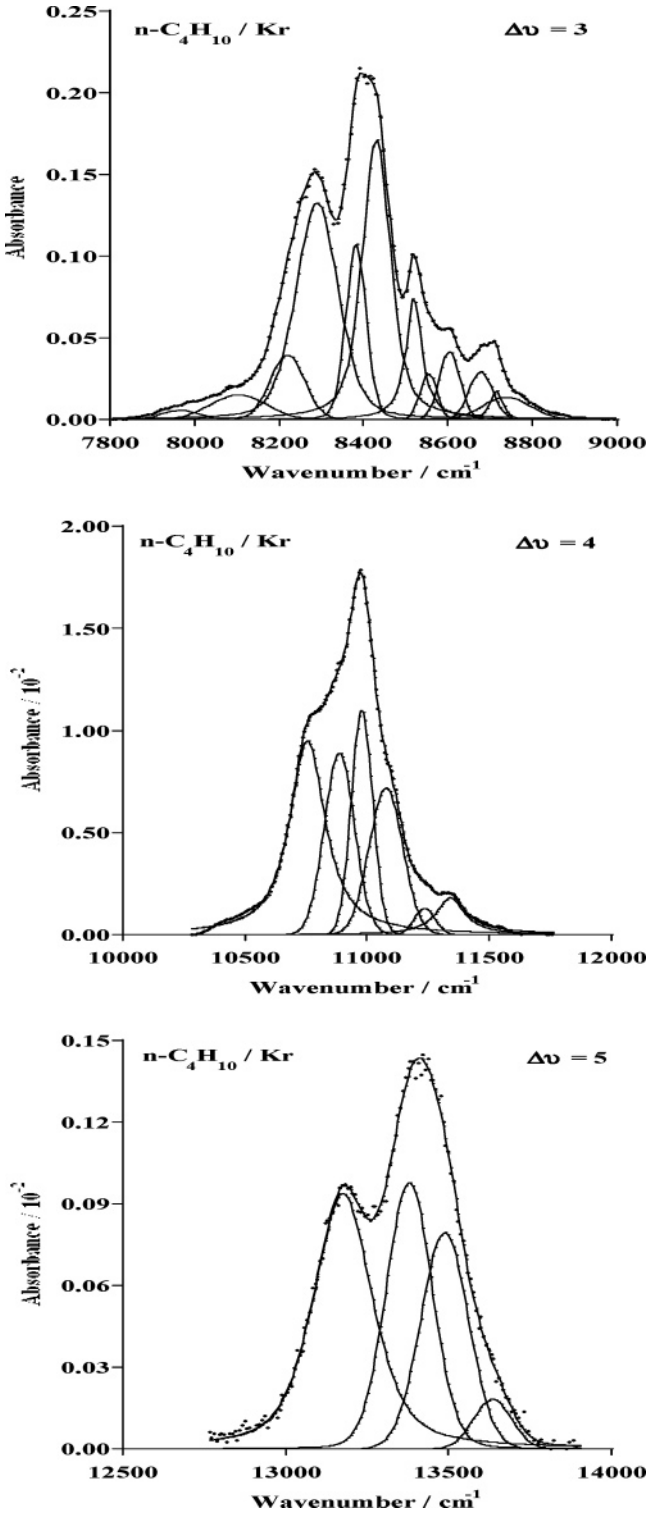

Figure 7. Selected absorption regions of vibrational C−H overtone spectra ($\Delta v = 3, 4, 5$) of *n*-C_4H_{10} in liquid krypton solution (2.2%) at 120 K.

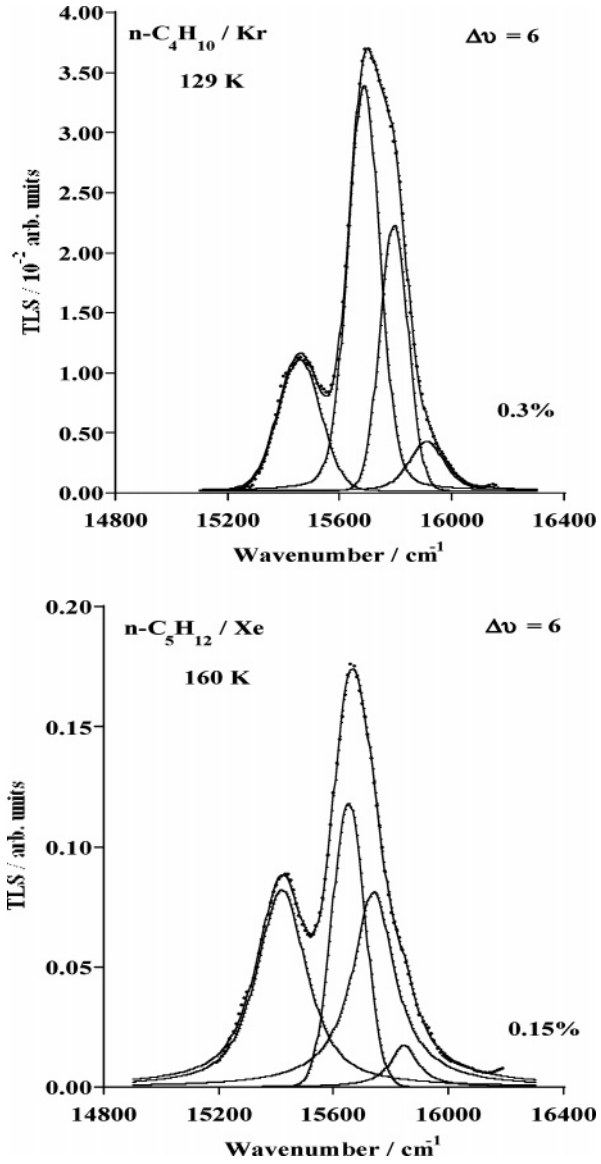

Figure 8. Thermal lens C−H ($\Delta v = 6$) spectrum of *n*-C_4H_{10} in liquid krypton solution (0.3%) at 129 K (top). Thermal lens C−H ($\Delta v = 6$) spectrum of *n*-C_5H_{12} in liquid xenon solution (0.15%) at 160 K (bottom).

al.,[26,27] methylene C−H bonds exhibit lower energy because of increased repulsive interactions. They also indicate that methyl groups exert an "inductive effect" on trans C−H bonds, increasing their vibrational frequency. This explains the energy order given above, since $C-H_{ip}$ is trans to a methyl group. Experimental energies were obtained by deconvolution, taking as reference the gas-phase study reported by Henry et al.[25] In all cases, the process was carried out using Lorentzian band shapes with a small Gaussian contribution. The same number of bands presented by Henry et al. was used to fit the third and fifth overtones. A higher number was required to accurately fit the second overtone. Clear shoulders on the spectrum suggested 11 bands rather than eight. Enhancement of spectral features in this region was also observed in ethane. The C−H ($\Delta v = 5$) spectrum was deconvoluted with three bands rather than five; increased noise in such a low absorption (0.002 au) is responsible for loss of spectral detail. The fifth overtone ($\Delta v = 6$) was obtained with the thermal lens technique. Figure 5 shows the spectrum of C_3H_8 (0.6%)−Ar at 93 K, where the excitation power was 60 mW and the chopping frequency 10 Hz. The C−H ($\Delta v = 6$) TLS spectrum of the pure liquid was also recorded, and the deconvoluted band is presented in Figure 5. Transition frequencies of the individual oscillators are $C-H_m$ (15 415), $C-H_{op}$ (15 613), and $C-H_{ip}$ (15 776 cm^{-1}). The corresponding bandwidths are 213, 210, and 202 cm^{-1}, respectively.

***n*-Butane.** The overtone spectra of *n*-C_4H_{10} (0.8%)−Kr and $HC(CH_3)_3$ (1.0%)−Kr at 120 K are shown in Figure 6. Since the solubility of butane and isobutane is very low in liquid argon, krypton was chosen as solvent to prepare a solution in which the fourth ($\Delta v = 5$) overtone could be observed. As previously indicated for propane, three different C−H oscillators ($C-H_m$,

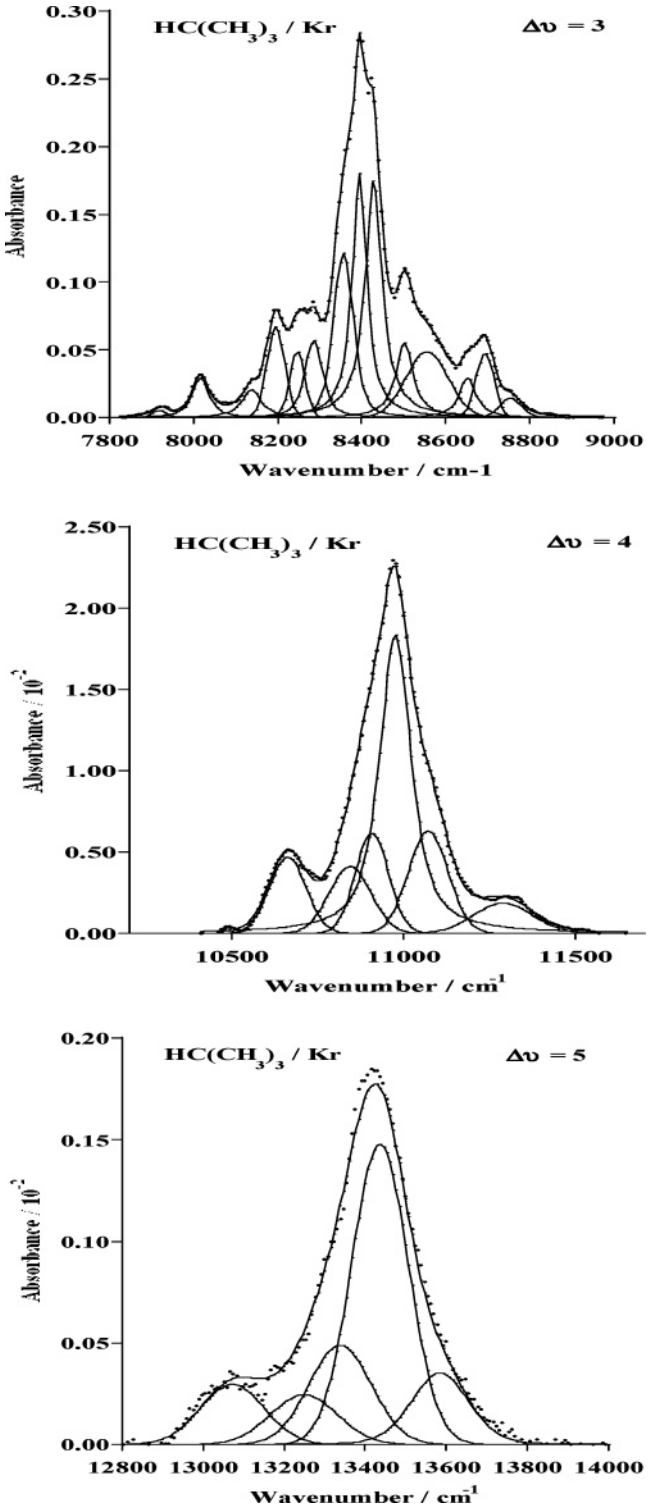

Figure 9. Selected absorption regions of vibrational C−H overtone spectra ($\Delta v = 3, 4, 5$) of $HC(CH_3)_3$ (1.0%) in liquid krypton at 120 K.

C−H_{op}, C−H_{ip}) make up the overtone bands. Once again, deconvolution was necessary to isolate each contribution and determine its vibrational frequency. Individual overtone regions are presented in Figure 7. The same number of bands used by Henry et al.[25] was used in the deconvolution of the third, fourth, and fifth overtones; however, the second required 12 bands rather than eight. Enhancement of spectral features was also observed in this region for ethane and propane. The thermal lens spectrum of *n*-C_4H_{10} (0.3%)−Kr at 129 K is shown in Figure 8. Excellent spectral quality allowed identification of each oscillator band.

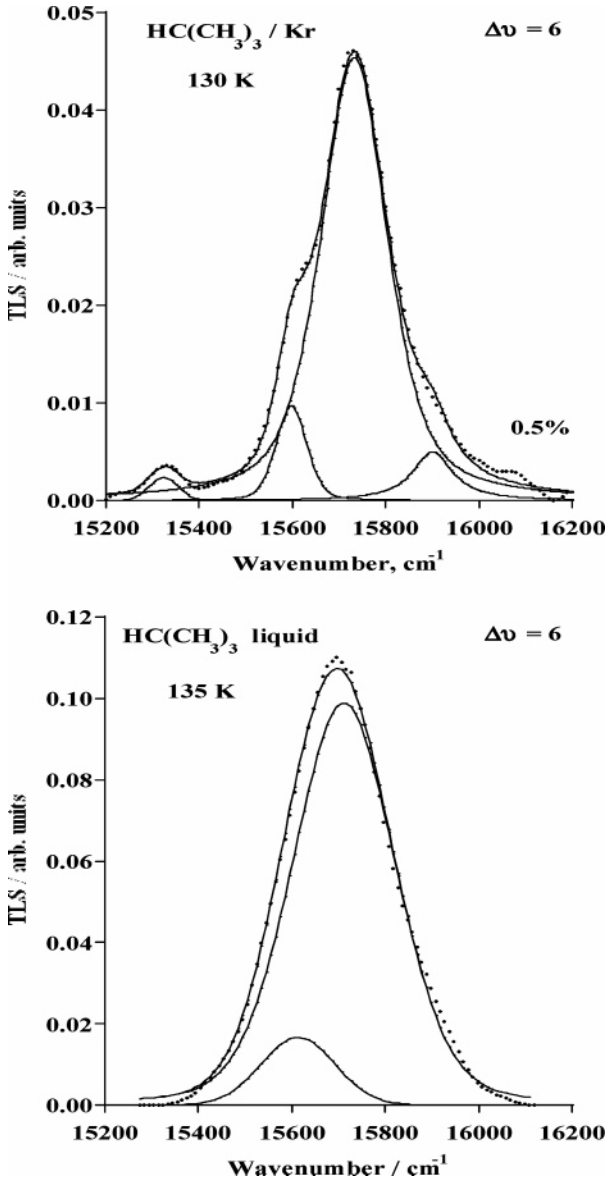

Figure 10. Thermal lens C−H ($\Delta v = 6$) spectrum of $HC(CH_3)_3$ in liquid krypton solution (0.5%) at 130 K (top). Thermal lens C−H ($\Delta v = 6$) spectrum of liquid $HC(CH_3)_3$ at 135 K (bottom).

***n*-Pentane.** To complete a hydrocarbon series, the C−H ($\Delta v = 6$) TLS spectrum of pentane dissolved in liquid xenon was also recorded and presented in Figure 8. Xenon was chosen as solvent because the solubility of pentane in argon and krypton is lower than that for xenon. The gas mixture was condensed at 165 K, and its concentration was estimated to be 0.15%. The excitation power used in the experiment was 200 mW and the chopping frequency 0.50 Hz. Low chopping frequency was necessary to avoid saturation of the thermal lens signal. Reduced thermal conductivity of liquid xenon is believed to be responsible. The classification of C−H oscillators is the same used for propane and butane. Experimental frequencies (cm^{-1}) and bandwidths ($\Delta\omega_{1/2}$) in solution are: C−H_m 15 420 (207 cm^{-1}), C−H_{op} 15 652 (136 cm^{-1}), and C−H_{ip} 15 739 (179 cm^{-1}).

Isobutane. Figure 9 shows the main overtone bands of isobutane ($HC(CH_3)_3$) dissolved in liquid krypton at 120 K. The concentration of the sample was estimated to be 1.0%. Since the geometry of the molecule varies from propane and butane, a different classification is given to C−H oscillators. The oscillator of lowest energy is labeled C−H_t and corresponds to the only tertiary C−H bond in isobutane. The other two

TABLE 1: Experimental Vibrational Overtone Absorptions and Bandwidths ($\Delta\omega_{1/2}$) of C_2H_6 in Gas Phase, Liquid Argon Solution, and Liquid Phase (cm^{-1})[a]

Δv	obsd (gas)/ ($\Delta\omega_{1/2}$)	$\Delta\omega_{gas-solution}$	obsd (liquid Ar)/($\Delta\omega_{1/2}$)	$\Delta\omega_{gas-liquid}$	obsd (liquid)/ ($\Delta\omega_{1/2}$)
3	8459/(100)	19	8440/(67)	36	8423/(72)
4	11047/(153)	10	11037/(160)	39	11008/(171)
5	13490/(138)	41	13449/(196)	65	13425/(181)
6	15823/(131)	48	15775/(270)	77	15746/(180)
6		47	15776/(185) liquid N_2		
ω_e	3066 ± 5		3065 ± 11		3057 ± 8
$\omega_e x_e$	-61.8 ± 1.0		-62.2 ± 2.0		-61.7 ± 1.5
D_e	-38027		-37758		-37866

[a] Frequency shifts ($\Delta\omega$) gas−solution and gas−liquid. Local modes (ω_e), anharmonicities ($\omega_e x_e$), and dissociation energies (D_e).

TABLE 2: Experimental Vibrational Overtone Absorptions (cm^{-1}) and Bandwidths ($\Delta\omega_{1/2}$) of C_3H_8 in Gas Phase at 295 K and in Liquid Argon Solution at 92 K[a]

	Δv	obsd (gas)/ ($\Delta\omega_{1/2}$)	$\Delta\omega_{gas-solution}$	obsd (liquid Ar)/ ($\Delta\omega_{1/2}$)
CH_2 (C−H_m)	3	8340/(92)	33	8307/(115)
	4	10914/(111)	139	10775/(139)
	5	13302/(92)	89	13213/(147)
	6	15573/(128)	81	15492/(230)
	ω_e	3036 ± 10		3009 ± 18
	$\omega_e x_e$	62.9 ± 1.5		61.2 ± 3.3
	D_e	-36635		-36986
CH_3 (C−H_{op})	3	8435/(84)	35	8400/(56)
	4	10982/(106)	82	10900/(127)
	5	13419/(102)	22	13397/(201)
	6	15740/(93)	52	15688/(220)
	ω_e	3052 ± 7	16	3036 ± 20
	$\omega_e x_e$	61.0 ± 1.1		60.2 ± 3.5
	D_e	-38175		-38278
CH_3 (C−H_{ip})	3	8472/(55)	24	8448/(55)
	4	11040/(130)	48	10992/(114)
	5	13482/(85)		13495/(253)
	6	15830/(126)	36	15794/(281)
	ω_e	3060 ± 9		3055 ± 13
	$\omega_e x_e$	59.9 ± 1.4		60.2 ± 2.4
	D_e	-39080		-38758

[a] Frequency shifts ($\Delta\omega$) gas−solution. Local modes (ω_e), anharmonicities ($\omega_e x_e$), and dissociation energies (D_e).

oscillators are found in methyl groups. One bond (C−H_{ip}) lies in the same plane of the C−C bond, and the other (C−H_{op}) lies out-of-plane. Their energy order is known to be C−H_{ip} < C−H_{op},[13] which can be explained by the trans effect of methyl groups described by McKean et al.[26,27] Specifications for each deconvolution were taken from a previous report by Manzanares et al.[15] The C−H ($\Delta v = 6$) TLS spectrum of $HC(CH_3)_3$ (0.5%)−Kr at 130 K is shown in Figure 10. The excitation power was 60 mW and the chopping frequency 5.0 Hz. Deconvolution was carried out using four bands, taking as reference the C−H ($\Delta v = 5$) gas-phase spectrum reported by Lewis et al.[22] Two oscillators were clearly identified in our spectrum. The very weak C−H_t was not identified for all levels. The fifth overtone of liquid isobutane was also recorded at low temperature. The corresponding spectrum is shown in Figure 10. The weakest absorption C−H_t could not be observed.

4. Discussion

A summary of overtone frequencies and local-mode parameters of C_2H_6 is presented in Table 1. Local-mode parameters were calculated from a Birge−Sponer plot of the experimental data. Transition energies for the gas phase reported by Lewis et al.[23] and Henry and Greenlay[24] are also included to support peak assignments. The frequency shifts of gas−solution and gas−liquid are presented, as well as the fwhm. As expected, the gas−solution frequency shifts ($\Delta\omega$) are positive (red-shifted) and smaller than the gas−liquid shifts. The fwhm ($\Delta\omega_{1/2}$) values of the liquid and solution bands are similar except for $\Delta v = 6$ where the order is pure liquid (180 cm^{-1}) similar to liquid N_2 (185 cm^{-1}) and smaller than in liquid Ar solution (275 cm^{-1}). Calculated local-mode parameters are also included in Table 1. Since experimental liquid Ar solution and gas-phase results are very close, it is reasonable to conclude that vibrational energy levels of ethane do not suffer significant perturbation in liquid argon but interactions are shown through the bandwidths ($\Delta\omega_{1/2}$) in pure liquid and liquid argon solutions. Bandwidths are dependent on the vibrational level excited. Increased solute−

TABLE 3: Experimental Vibrational Overtone Absorptions (cm^{-1}) and Bandwidths ($\Delta\omega_{1/2}$) of *n*-C_4H_{10} in Gas Phase at 295 K and in Liquid Krypton Solution at 120 K[a]

	Δv	obsd (gas)/ ($\Delta\omega_{1/2}$)	$\Delta\omega_{gas-solution}$	obsd (liquid Kr)/ ($\Delta\omega_{1/2}$)
CH_2 (C−H_m)	3	8305/(125)	15	8290/(118)
	4	10781/(119)	25	10756/(176)
	5	13184/(122)	8	13176/(214)
	6	15466/(135)	11	15455/(175)
	ω_e	3017 ± 2		3004 ± 17
	$\omega_e x_e$	62.2 ± 0.3		61.5 ± 2.9
	D_e	-36585		-36683
CH_3 (C−H_{op})	3	8419/(77)	36	8383/(57)
	4	10987/(144)	100	10887/(145)
	5	13430/(149)	50	13380/(166)
	6	15752/(130)	63	15689/(138)
	ω_e	3050 ± 1		3022 ± 19
	$\omega_e x_e$	60.7 ± 0.2		58.3 ± 3.4
	D_e	-38313		-39162
CH_3 (C−H_{ip})	3	8455/(55)	24	8431/(79)
	4	11035/(72)	55	10980/(102)
	5	13515/(83)	27	13488/(172)
	6	15852/(107)	55	15797/(115)
	ω_e	3057 ± 3		3039 ± 14
	$\omega_e x_e$	59.4 ± 0.6		57.8 ± 2.5
	D_e	-39332		-39946

[a] Frequency shifts ($\Delta\omega$) gas−solution. Local modes (ω_e), anharmonicities ($\omega_e x_e$), and dissociation energies (D_e).

TABLE 4: Experimental Vibrational Overtone Absorptions (cm^{-1}) and Bandwidths ($\Delta\omega_{1/2}$) of $HC(CH_3)_3$ in Gas Phase at 295 K and in Liquid Krypton Solution at 120 K[a]

	Δv	obsd (gas)/ ($\Delta\omega_{1/2}$)	$\Delta\omega_{gas-solution}$	obsd (liquid Kr)/ ($\Delta\omega_{1/2}$)
C−H_t	3	8324	38	8286/(50)
	4	10853	9	10844/(143)
	5	13240	−8	13248/(194)
	6	15305	−19	15324/(74)
	ω_e	3018 ± 4		3016 ± 10
	$\omega_e x_e$	61.3 ± 0.9		61.0 ± 1.5
	D_e	-37147		-37280
C−H_{op}	3	8451	23	8428/(49)
	4	11005	29	10976/(111)
	5	13460	24	13436/(164)
	6	15804/(75)	71	15733/(170)
	ω_e	3065 ± 3		3055 ± 9
	$\omega_e x_e$	62.1 ± 0.8		61.6 ± 1.6
	D_e	-37819		-37878
C−H_{ip}	3	8376	19	8357/(56)
	4	10930	22	10908/(114)
	5	13355	17	13338/(181)
	6	15683/(102)	85	15598/(78)
	ω_e	3045 ± 4		3034 ± 9
	$\omega_e x_e$	62.0 ± 1.1		61.7 ± 1.6
	D_e	-37387		-37298

[a] Frequency shifts ($\Delta\omega$) gas−solution. Local modes (ω_e), anharmonicities ($\omega_e x_e$), and dissociation energies (D_e).

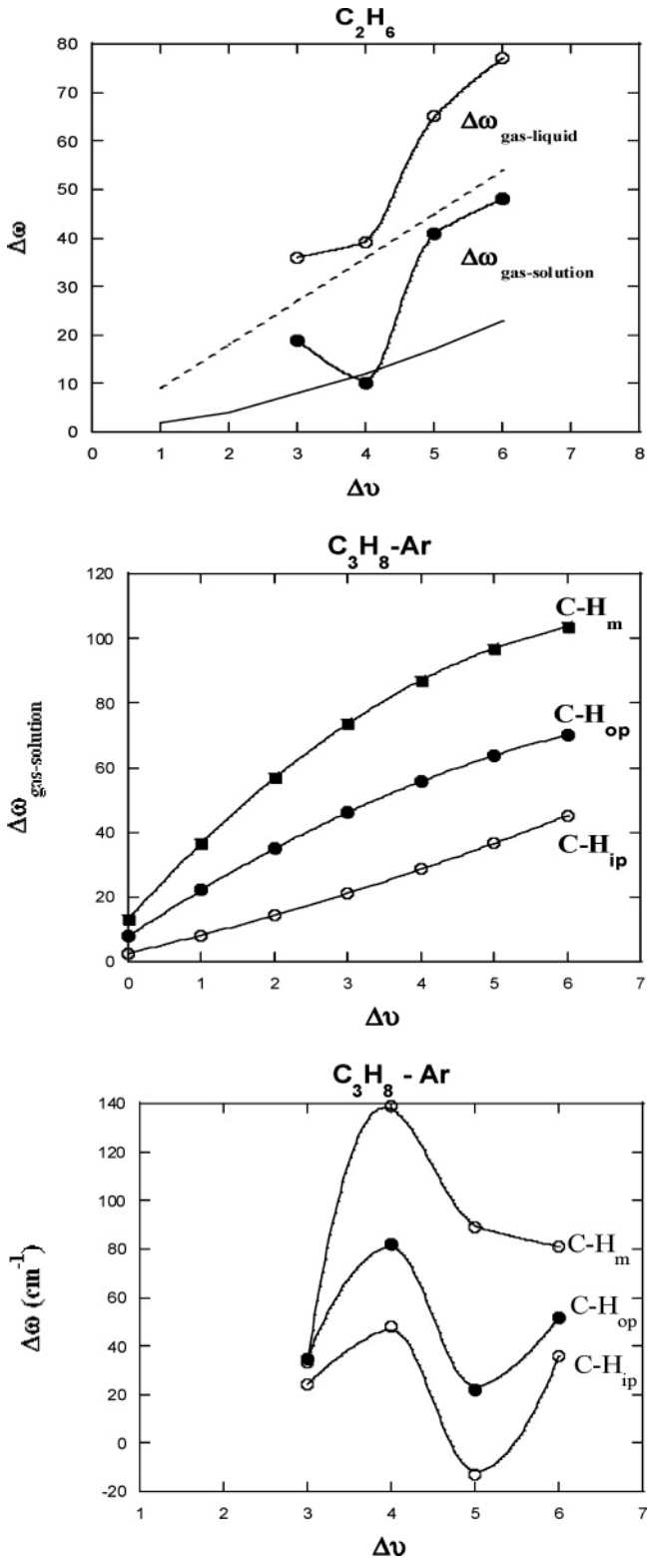

Figure 11. Experimental (circles) and calculated (lines) frequency shift ($\Delta\omega$) gas−liquid and gas−solution for C_2H_6 (top). Calculated ($\Delta\omega$) for C_3H_8–Ar for three different oscillators (middle) and experimental gas−solution ($\Delta\omega$) for C_3H_8–Ar (bottom) for three different oscillators.

solute and solute−solvent interactions are known to be responsible.[28−30]

Table 2 shows experimental frequencies of C_3H_8. As expected, frequencies in solution are red-shifted in comparison to that in gas phase. Intermolecular interactions between solute and solvent are known to be responsible.[28,31] The increase in

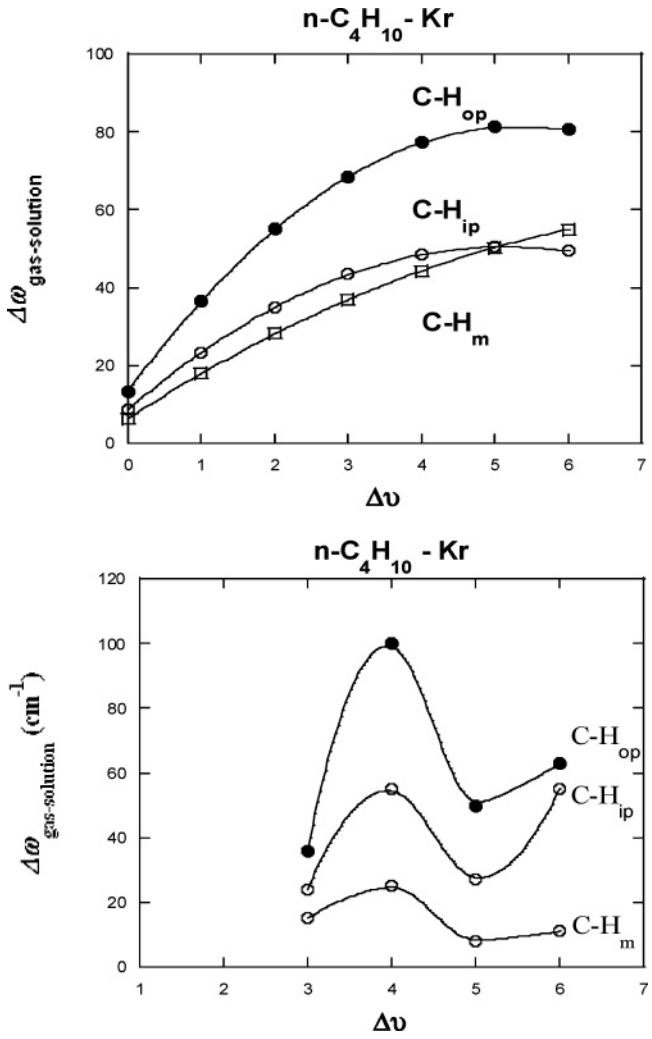

Figure 12. Calculated (top) and experimental (bottom) gas−solution frequency shift ($\Delta\omega$) for three different oscillators of *n*-C_4H_{10} dissolved in Kr.

bandwidths is a direct consequence of such interactions. The Birge−Sponer plot for each oscillator in propane produced the local-mode parameters shown in Table 2, along with gas-phase determinations by Henry et al.[25] Both harmonic frequency and anharmonicity appear to be lower in solution; although experimental uncertainty suggests no statistical difference. Similar trends in anharmonicity are observed in both cases. $C-H_m$ oscillators have the highest value while $C-H_{ip}$ the lowest. Since solvation in nonpolar solvents is not expected to modify the chemical environment of the C−H bonds, the relative order in anharmonicity should also remain unchanged.

Corresponding transition frequencies are presented in Table 3, along with gas-phase results. Using the information in Table 3, we constructed Birge−Sponer plots for the C−H oscillators; local-mode parameters are summarized in Table 3. Harmonic frequencies are red-shifted in solution, and anharmonicities follow the same trend as those in gas phase. There is no statistical difference between solution and gas-phase values; however, the consistent red-shift in vibrational energies suggests that harmonic frequencies are indeed lower in solution. Regarding anharmonicities, the gap between results is too small to reach a similar conclusion.

Vibrational frequencies and bandwidths are summarized in Table 4. For isobutane, local-mode parameters from Birge−Sponer plots are also summarized in Table 4. In general,

TABLE 5: Fifth Overtone ($\Delta v = 6$) Bandwidth of C_2H_6 in Solution: C_2H_6−Ar (92 K), C_2H_6–N_2 (85 K), and Liquid C_2H_6 (100 K)

Solvent Properties[a]				
solvent	T (K)	σ (pm)	$\rho/(10^{22}$ cm$^{-3})$	$\rho^{-1/3}/(10^{-8}$ cm)
Ar	92	341.8	2.1216	3.6122
N_2	85	368.1	1.7386	3.8601
C_2H_6	100	430.7	1.2835	4.2711

Solvent Refractive Index and $[(\Delta\omega_{1/2})_{solution}/(\Delta\omega_{1/2})_{gas}] = A = n(n^2+2)^2/9$[b]						
solution	T (K)	n	$(\Delta\omega_{1/2})_{solution}$	$(\Delta\omega_{1/2})_{gas}$	A_{expt}	A_{calcd}
C_2H_6–Ar	92	1.226	270	131	2.0611	1.6717
C_2H_6–N_2	85	1.197	185	131	1.4122	1.5674
C_2H_6–C_2H_6	100	1.388	180	131	1.3740	2.3759

Solute Lennard-Jones Effective Parameter (σ_{expt}) in Solution[c]					
solution	T (K)	$u/$(cm s^{-1})	$(\Delta\omega_{1/2})_{solution}$	σ_{expt} (pm)	σ_{calcd} (pm)
C_2H_6–Ar	92	33686	270	356	387
C_2H_6–N_2	85	35221	185	379	399
C_2H_6–C_2H_6	100	37516	180	419	431

[a] Solvent properties: Density (ρ) and Lennard-Jones (σ) parameter. [b] Calculated and experimental ratio of bandwidths in solution and gas phase using the index of refraction of the solvent (n). [c] Calculated and experimental Lennard-Jones effective parameter (σ) using the binary collision model, average thermal velocity (u), and bandwidth ($\Delta\omega_{1/2}$) in cm^{-1}.

excellent fitting was obtained in the Birge−Sponer plots of C−H_{ip} and C−H_{op}; however, C−H_t points showed dispersion. This issue is attributed to the uncertain deconvolution of such a weak band. The assignment of this band was originally made by Wong and Moore;[32] however, calculations made by Manzanares et al.[15] suggest that it is a combination band rather than an overtone. For this reason, the data point was not included in the linear fit. Local-mode parameters in krypton solution closely agree with reported values in pure liquid. The only exception is the harmonic frequency of C−H_t, for which uncertainty is higher for reasons previously mentioned. Even though anharmonicities seem lower in solution, fitting errors indicate that there is no statistical difference with respect to that in pure liquid.

4.1. Frequency Shifts. The differences in peak absorption frequencies between the C−H gas phase and the C−H in solution absorptions are presented in Figure 11. A possible qualitative explanation for the results is based on the local-mode parameters for one-dimensional C−H oscillator. The transition energies associated with local-mode overtones are described by the two-parameter equation:

$$(\Delta E/v) = \omega_e - \omega_e x_e (v+1) \qquad (1)$$

The local-mode parameters (ω_e and $\omega_e x_e$) are used to calculate the dissociation energy (D_e) using the equation $D_e = -\omega_e^2/4\omega_e x_e$, and the potential energy curve is represented by the Morse oscillator equation: $V(r) = D_e\{1 - \exp[-\beta(r - r_e)]\}^2$, where r_e is the location of the minimum and β is a parameter that controls the width of the potential.

Tables 1−4 show the calculated local-mode parameters for C−H bonds of C_2H_6, C_3H_8, and n-C_4H_{10}. Figure 11 (top) shows that the experimental $\Delta\omega_{gas-liquid}$ (open circles) values are larger than the $\Delta\omega_{gas-solution}$ (solid circles) values. In the first approximation, the frequency shift gas−liquid and gas−solution can be predicted using the differences between harmonic frequencies. For example, Table 1 shows that the shift ($\Delta\omega$) gas−solution for ethane is smaller (1 cm^{-1}) than the difference gas−liquid (9 cm^{-1}). Calculated differences using eq 1 and respective gas phase, liquid, and solution harmonic frequencies and anharmonicities are also shown in Figure 11 (top) where the difference gas−liquid is indicated by a broken line and the difference gas−solution is indicated by a solid line. These two lines predict gas−liquid differences that are always larger than gas−solution. Figure 11 (middle) shows $\Delta\omega_{gas-solution}$ calculated using eq 1 for three different types of C−H bonds in C−H. The calculation indicates that the differences are always in the order C−H_m > C−H_{op} > C−H_{ip}. The experimental differences are presented in Figure 11 (bottom). Ignoring the oscillations of the experimental results, we show that the prediction shown in the middle of Figure 11 is correct. This kind of prediction is not limited to ethane and propane. In the case of *n*-butane, the prediction is that the differences are in the order C−H_{op} > C−H_{ip} > C−H_m; this is the order shown experimentally in Figure 12 except for transitions to levels 5 and 6 of C−H_{ip} and C−H_m. Predictions for C−H_{op} slightly larger than C−H_{ip} of isobutane are similar to experimental results except for $\Delta v = 6$. Calculated values for C−H_t of isobutene cannot be compared with experimental results because the peak position of the C−H_t band is based on unreliable deconvolution of a small band. For the molecules studied, the actual experimental values of $\Delta\omega_{gas-solution}$ are more complicated than the simple model prediction because they depend on the overtone levels involved as well as their interactions with other vibrational levels.

4.2. Bandwidths. The ratio of relaxation time in solution with respect to relaxation time in the gas phase ($\tau_{solution}/\tau_{gas}$) is equal to the inverse of the ratio of bandwidths $(\Delta\omega_{1/2})_{solution}/(\Delta\omega_{1/2})_{gas}$ and is related to the index of refraction of the solvent[33] through the equation $(\tau_{solution}/\tau_{gas}) = 9/n(n^2+2)$.[2] The results of the calculation for ethane in solution are shown in the middle of Table 5. The tendency of ratios calculated using experimental results is the opposite to the ratios calculated using indexes of refraction of the solvents. It is concluded that the bandwidths are not the result of changes in the index of refraction of each solvent.

Another analysis of the bandwidths of ethane in solution is based on collisions between ethane and the solvent. The isolated binary collision (IBC) model for vibrational relaxation in liquids was developed by Litovitz and co-workers.[34,35] The vibrational relaxation rate (k) is related to the transition probability from initial level (i) to final level (f) in the molecule (P_{fi}) and the collision rate (k_c) through the equation $k = P_{fi}k_c$. To calculate

the collision rate, the cell model is used. The central molecule of effective diameter (σ) moves a distance ($\rho^{-1/3} - \sigma$) between collisions at average thermal velocity $u = (8RT/\pi M)^{1/2}$. The relaxation rate is proportional to the bandwidth ($\Delta\omega_{1/2}$) through the equation $k = 2\pi c\Delta\omega_{1/2}$. Usually, $\Delta\omega_{1/2}$ is obtained experimentally for several solvents at the same temperature. The collision frequency is very sensitive to the choice of σ, and the arithmetic average of reported values of σ from solute and solvent is usually larger than $\rho^{-1/3}$. The procedure frequently used is to plot k versus $\rho^{-1/3}$ for different solvents at a common temperature. Confirmation of the model is obtained if the points lie on a straight line and σ is comparable to the σ value reported from gas-phase virial or transport data.

Our bandwidth measurements are for ($\Delta v = 6$) transitions of C_2H_6 in different solvents at different temperatures. This is not the case described before to test the IBC model, but for our results the IBC model was used in the following way. To determine the possible origin of the bandwidth, we arbitrarily assume that $2\pi c\Delta\omega_{1/2} = k_c$ and the effective diameter is calculated from the equation:

$$\sigma = \frac{1}{\rho^{1/3}} - \frac{u}{2\pi c\Delta\omega_{1/2}} \qquad (2)$$

Table 5 (bottom) shows the results of the calculated effective diameter using eq 2 (σ_{expt}) and the arithmetic average (σ_{calcd}) of the diameters calculated from transport data. There is an obvious linear correlation between the two values, indicating the possibility that binary collisions are responsible for the observed bandwidth of the $\Delta v = 6$ overtone transition in C_2H_6. To obtain the estimated σ values, it was assumed that the probability P_{fi} is the same ($v_i = 6$ and v_f is not known) for all solvents and arbitrarily made equal to 1.

5. Conclusions

The application of the thermal lens technique to cryogenic solutions has been demonstrated with the study of ethane in liquid Ar, N_2, and pure liquid, propane in liquid Ar, *n*-butane and isobutane in liquid Kr, and pentane dissolved in liquid Xe. As shown for liquids at room temperature, the sensitivity of the technique is high enough to obtain high vibrational overtones of molecules and to detect the weak absorptions in dilute cryogenic solutions. Small frequency shifts are detected indicating the relatively small changes in harmonic frequencies and anharmonicities from gas-phase absorption to solute molecules surrounded by cryogenic solvents. Absorption bandwidths are influenced by the change in solvent. In the case of ethane, bandwidths seem to correlate with the effective diameter of the collision pair. The hydrocarbon concentration in solution between 0.1 and 1% is still too high to show pure monomer absorption. The spectra are probably the result of absorption by monomers, dimers, and some larger clusters in solution. More sensitive methods are underway in our laboratory to observe the absorptions at lower concentrations.

Acknowledgment. This work was supported by the Robert A. Welch Foundation under Grant No. AA-1173. Partial support is also acknowledged from the Baylor University Research Committee.

References and Notes

(1) Bulanin, M. Liquefied Gases as Solvents for Vibrational Spectroscopy. In *Handbook of Vibrational Spectroscopy;* Chalmers, J., Griffiths, P., Eds.; Wiley & Sons: New York, 2001; pp 1329−1341.

(2) Clark, R.; Hester, R. *Molecular Cryospectroscopy;* Wiley & Sons: New York, 1995; pp 1−120, 176−240.

(3) Navea, J.; Lopez-Calvo, A.; Manzanares, C. Thermal Lens Spectroscopy in Liquid Argon Solutions: ($\Delta v = 6$) CH Vibrational Overtone Absorption of Methane. *J. Phys. Chem. A* **2006**, *110*, 1594−1599.

(4) Lopez-Calvo, A.; Manzanares, C. E. Thermal Lens Spectroscopy in Cryogenic Solutions: Analysis and Comparison of Intensities in CH_4-N_2 and CH_4-Ar Liquid Solutions. *J. Phys. Chem. A* **2006**, *110*, 10427−10434.

(5) Swofford, R.; Long, M.; Albrecht, A. C-H Vibrational States of Benzene, Naphthalene, and Anthracene in the Visible Region by Thermal Lensing Spectroscopy and the Local Mode Model. *J. Chem. Phys.* **1976**, *65*, 179−190.

(6) Swofford, R.; Long, M.; Albrecht, A. Thermal Lens Technique: A New Method of Absorption Spectroscopy. *Science* **1976**, *191*, 183−185.

(7) Patel, C.; Nelson, E.; Kerl, R. Opto-acoustic Study of Weak Optical Absorption on Liquid Methane. *Nature* **1980**, *286*, 368−370.

(8) Nelson, E.; Patel, C. Visible Absorption Spectrum of Liquid Ethylene. *Proc. Natl. Acad. Sci. U.S.A.* **1981**, *78*, 702−705.

(9) Patel, C.; Nelson, E.; Kerl, R. Vibrational Overtone Absorption in Solid Hydrogen. *Phys. Rev. Lett.* **1981**, *47*, 1631−1635.

(10) Glatt, I.; Kerl, R.; Patel, C. Observation of the Fourth Vibrational Overtone of Hydrogen. *Phys. Rev. Lett.* **1986**, *57*, 1437−1439.

(11) Blunt, V.; Cedeño, D.; Manzanares, C. Vibrational Overtone Spectroscopy of Methane in Liquid Argon Solutions. *Mol. Phys.* **1997**, *91*, 3−17.

(12) Blunt, V.; Brock, A.; Manzanares, C. Overtone Spectroscopy of CHD_3 in Liquid Argon Solutions. *Ber. Bunsen-Ges.* **1995**, *99*, 520−529.

(13) Blunt, V.; Brock, A.; Manzanares, C. Near-Infrared and Visible Spectroscopy of CH_3D in Liquid Argon Solutions. *J. Phys. Chem.* **1996**, *100*, 4413−4419.

(14) Brock, A.; Mina-Camilde, N.; Manzanares, C. Vibrational Spectroscopy of C-H Bonds of C_2H_4 Liquid and C_2H_4 in Liquid Argon Solutions. *J. Phys. Chem.* **1994**, *98*, 4800−4808.

(15) Manzanares, C.; Peng, J.; Mina-Camilde, N.; Brock, A. Overtone Spectroscopy of Isobutane at Cryogenic Temperatures. *Chem. Phys.* **1995**, *190*, 247−259.

(16) Manzanares, C.; Camilde-Mina, N.; Brock, A.; Peng, J.; Blunt, V. Piezoelectric Detection of Vibrational Overtones at Cryogenic Temperatures. *Rev. Sci. Instrum.* **1995**, *66*, 2644−2651.

(17) Onsager, L. Electric Moments of Molecules. *J. Am. Chem. Soc.* **1938**, *58*, 1486−1493.

(18) Kirkwood, J. G. Theory of Solutions of Molecules Containing Widely Separated Charges with Special Application to Zwitterions. *J. Chem. Phys.* **1934**, *2*, 351−361.

(19) Jara, H.; Pummer, H.; Egger, H.; Shahidi, M.; Rhodes, C. K. Interaction of Rare-Gas-Halide Excimers with Simple Cryogenic Liquids. *Phys. Rev. B* **1986**, *34*, 7534−7541.

(20) Momose, T.; Miki, M.; Wakabayashi, T.; Shida, T.; Chan, M. C.; Lee, S. S.; Oka, T. Infrared Spectroscopic Study of Rovibrational States of Methane Trapped in Parahydrogen Crystal. *J. Chem. Phys.* **1997**, *107*, 7707−7716.

(21) Momose, T.; Katsuki, H.; Hoshina, H.; Sogoshi, N.; Wakabayashi, T.; Shida, T. High Resolution Laser Spectroscopy of Methane Clusters Trapped in Solid Parahydrogen. *J. Chem. Phys.* **1997**, *107*, 7717−7720.

(22) Lewis, E.; Moehnke, C.; Manzanares, C. Phase Shift Cavity Ring Down and FT-VIS Measurements of C-H ($\Delta v = 5$) Vibrational Overtone Absorptions. *Chem. Phys. Lett.* **2004**, *394*, 25−31.

(23) Lewis, E.; Reynolds, D.; Li, X.; de Villele, G.; Leduc, C.; Cedeño, D.; Manzanares, C. Phase Shift Cavity Ring-Down Measurement of C-H ($\Delta v = 6$) Vibrational Overtone Absorptions. *Chem. Phys. Lett.* **2001**, *334*, 357−364.

(24) Henry, B.; Greenlay, R. Detailed Features in the Local Mode Overtone Bands of Ethane, Neopentane, Tetramethylbutane, and Hexamethylbenzene. *J. Chem. Phys.* **1980**, *72*, 5516−5524.

(25) Kjaergaard, H.; Hengtai, Y.; Bernhard, S.; Henry, B. Intensities in Local Mode Overtone Spectra: Propane. *J. Chem. Phys.* **1990**, *93*, 6239−6248.

(26) McKean, D. Individual CH Bond Strengths in Simple Organic Compounds: Effects of Conformation and Substitution. *Chem. Soc. Rev.* **1978**, *7*, 399−422.

(27) McKean, D.; Biedermann, S.; Burger, H. CH Bond Lengths and Strengths, Unperturbed CH Stretching Frequencies, from Partial Deuteration Infrared Studies: t-Butyl Compounds and Propane. *Spectrochim. Acta, Part A* **1974**, *30*, 845−857.

(28) Pullin, A. A Theory of Solvents Effects in Infrared Spectra. *Proc. R. Soc. London, Ser. A* **1960**, *255*, 39−43.

(29) Bayliss, N.; Cole, A.; Little, L. Solvent Effects in Infrared Spectra: C=O, C-H, and C-C Vibrations. *Aust. J. Chem.* **1955**, *8*, 26−38.

(30) Jatkar, S.; Jatkar, V.; Mukhedkar, A. Solvent Effect on Infrared Spectra. *J. Indian Chem. Soc.* **1963**, *40*, 715−720.

(31) Oxtoby, D. Vibrational Relaxation in Liquids. *Annu. Rev. Phys. Chem.* **1981**, *32*, 77−101.

(32) Wong, J.; Moore, B. Inequivalent C-H Oscillators of Gaseous Alkanes and Alkenes in Laser Photoacoustic Overtone Spectroscopy. *J. Chem. Phys.* **1982**, *77*, 603−615.

(33) Legay, F. In *Chemical and Biochemical Applications of Lasers;* Moore, C. B., Ed.; Academic Press: New York, 1977; Vol. 2, pp 43−86.

(34) Herzfeld, K. F.; Litovitz, T. A. *Absorption and Dispersion of Ultrasonic Waves;* Academic Press: New York, 1959.

(35) Madigosky, W. M.; Litovitz, T. A. Mean Free Path and Ultrasonic Vibrational Relaxation in Liquids and Dense Gases. *J. Chem. Phys.* **1961**, *34*, 489−497.